

# **Geostatistic Analysis of Long-Term Subsidence Effects on Isostasy of Long Island Using Continuous GPS Displacement Rates Using R**

Parag, A. S.<sup>1</sup>, Marsellos, A.E.<sup>1</sup>, Tsakiri, K.G.<sup>2</sup>

<sup>1</sup>*Dept. Geology, Environment and Sustainability, Hofstra University, NY, USA.*

<sup>2</sup>*Dept. Information Systems, Analytics, and Supply Chain Management, Rider University, NJ, USA.*

*aparag1@pride.hofstra.edu*

## **Abstract**

Long Island has experienced subsidence since the last ice age when the large Laurentide ice sheet covered most of New York State and readjusted after it melted. This process of readjustment of the land is known as isostasy, the equilibrium position where a body of land should sit between the surface above and below. However, the region is not uplifting after the weight of the ice melted but rather continues to subside even after this event took place. Modern human environmental interferences, particularly groundwater overpumping, causes uneven land deformation that heightens risks of landslides, sinkholes, and other geohazards (U.S. Geological Survey, n.d.). Central Long Island, with its many residential properties, has a high demand for groundwater, leading to the overpumping of aquifers in certain areas. This excessive withdrawal may contribute to gradual subsidence in parts of the region. In contrast, areas within New York City and Montauk Point exhibit significant subsidence rates despite lower residential groundwater extraction. This is likely due to reliance on upstate water sources, heavy infrastructure, and high population density. While Montauk Point is less populated than central and western Long Island, it still experiences notable subsidence, possibly due to reduced aquifer pumping, which allows underlying geological formations to compact under their own weight. To capture these spatial variations in land motion, we analyzed continuous GPS records from multiple stations across differing time intervals. Rather than restricting our study to a common observation window, we considered each station's full operational timeline to assess overall trends. A GIS-interpolated map of average displacement rates reveals localized areas of significant subsidence, illuminating the combined effects of natural isostatic processes and human-induced stresses. Findings support the need for strategic groundwater management and infrastructure planning to reduce further land subsidence and its associated hazards in this vulnerable coastal setting.

## **Introduction**

Long Island experiences flooding often due to the subsidence of the land from past glacial events. When the ice lays upon the land it weighs it down causing the area to subside and the sea level to rise and expose the lower areas to the possibility of flooding. When the ice melts it goes into the surrounding waters and takes weight off the land causing the land to uplift and sea-level to rise. Isostasy takes its role to lift the land back to its equilibrium balance where there is an equal amount of land above and below to be stable. Extreme levels of subsidence or uplift in certain areas can cause an increased risk of flooding, landslides, and sinkholes. The amount of

submergence is proportional to the proximity of deep water (Bloom, 1967). Long Island continues to subside leading to increasing geohazard risks, therefore the idea behind this study is to determine the possible issues in the future by using the geostatistic analysis to reveal the oscillations in vertical displacement through long-term geostatistical analysis.

This research can reveal if subsidence throughout Long Island continues to occur after past studies between 2005-2020. Previous research about the isostasy of Long Island has only focused on the glacial isostatic adjustment (GIA) depicting the melting of Pleistocene ice sheets that causes certain areas to uplift while others subside, impacting those areas to be at high risk of flooding (Moore, 2023). However, in this study GPS data will be used to detect the continued vertical land movements where glacial isostatic adjustment was present to suggest that Long Island is experiencing significant subsiding and very little uplift in certain areas. Studies have shown that along the outer shores of Long Island the fluctuations in groundwater level may trigger groundwater vibrational long-term movements that cause underground erosion, leading to landslides (Badger, 2024). Geohazards like landslides contribute to land subsidence since there is an added weight to the compaction of sediment and less support within the land surface resulting in possible sinking. The formation of sinkholes similarly contributes to land subsidence because of the breakdown of underlying sediments collapsing within themselves due to groundwater movements (Hope, 2024). This study will provide an understanding of the contributing factors to the process of isostasy in Long Island while also providing the knowledge many researchers can use to prevent harm and damage to the environment and the people who live there.

## **Methods**

GPS displacement data were retrieved using the R programming language from the Nevada Geodetic Laboratory's Global GPS Network for 14 GPS stations across Long Island: MNP1, NYRH, MOR6, SG06, ZNY1, NYDP, NYCI, QYNS, NYQN, NYEL, NYJM, NYBK, NYBR, and NYCO. Data retrieval and preliminary processing were performed using the R packages: data.table, lubridate, dplyr, purrr, imputeTS, and zoo. Data.table package used for fast and memory-efficient data manipulation for large datasets. Lubridate is used to format dates. Dplyr is used for easier data manipulation. Purrr is used for more efficient tools. ImputeTS is used for time series imputation along with plotting and printing functions of time series missing data statistics. Zoo used for time-series analysis. A custom function (GPS\_dwd) was written to access and structure the GPS data, creating a unified dataset consisting of northward, eastward, and upward displacement components, formatted and visualized using RStudio.

Initial data cleaning involved identifying duplicate and missing dates within each dataset using R functions and subsequently filling these gaps through linear interpolation methods (na\_interpolation) from the imputeTS package. Stations MOR6 and QYNS were excluded due to significant data integrity issues, such as excessive outliers and missing data points identified during initial analyses, possibly due to an antenna change causing large gaps within the data set. Outliers within the dataset were detected and removed using Z-score normalization, calculated through custom R functions, with values exceeding  $\pm 3$  standard deviations being replaced by NA values.

A second round of interpolation was conducted to produce a continuous and sturdy data series. The GPS satellites transmit signals that pick up many atmospheric interferences which create noise within the GPS ground stations. To smooth out the data and remove some of that noise, a moving average was applied to zoom into the actual data and visualize those patterns provided by the vertical displacement graphs. Kolmogorov-Zurbenko (KZ) filtering was applied to the cleaned and interpolated datasets using the kza package with a 365-day moving window and three replications, revealed to smooth data within a global wavelet spectrum. This effectively minimized short-term atmospheric oscillations, highlighting meaningful long-term trends. The Kolmogorov-Zurbenko (KZ) filter is essential for improving data quality, particularly effective against short-term fluctuations, non-stationary data, and outliers, without causing signal distortion like a standard moving average might (Yang et al., 2010; Tsakiri & Zurbenko, 2011a; Tsakiri & Zurbenko, 2011b; Tsakiri et al., 2018). It operates through an iterative process that stabilizes output and enhances the identification and analysis of patterns and frequencies in noisy datasets. Notably, we applied a minimal window size and few iterations in our approach to prevent over-smoothing and maintain data integrity.

Wavelet analysis was conducted to identify periodic signals in the cleaned GPS time series for each station's Up, North, and East components. The WaveletComp package's `analyze.wavelet` function was then used ( $dt = 1$  day,  $dj = 1/24$ ) over periods spanning 20–2024 days, with significance testing based on 10 Monte Carlo simulations. The resulting power spectra were plotted to visualize dominant periodicities and their evolution over time, providing insights into both seasonal and longer-term trends in vertical displacement across Long Island's GPS stations (Figure 3). Vertical displacement rates were computed through linear regression modeling (`lm` function) of the smoothed data. To capture these spatial variations in land motion, we analyzed continuous GPS records from multiple stations across differing time spans. Rather than restricting our study to a common observation window, we considered each station's full operational timeline to assess overall trends. Spatial interpolation of displacement rates was performed using the Inverse Distance Weighting (IDW) method, implemented via the `gstat` and `sp` packages, generating a detailed spatial representation of subsidence across Long Island. The GIS (Geographical Information System) map with an interactive visualization of station locations and displacement rates was created using the `leaflet` package, enabling intuitive spatial interpretation of the findings.

## **Results**

The spatial analysis of vertical displacement rates across Long Island and New York City revealed distinct patterns of subsidence throughout Long Island. Notably, regions in proximity to New York City exhibited the highest subsidence rates, reaching values of approximately -2 millimeters per year (Figure 4). Eastern Long Island also displayed similar subsidence, although with slightly lower rates compared to the urban areas closer to New York City. The stations within Central Long Island revealed lower subsidence rates, often closer to neutral or minimal vertical

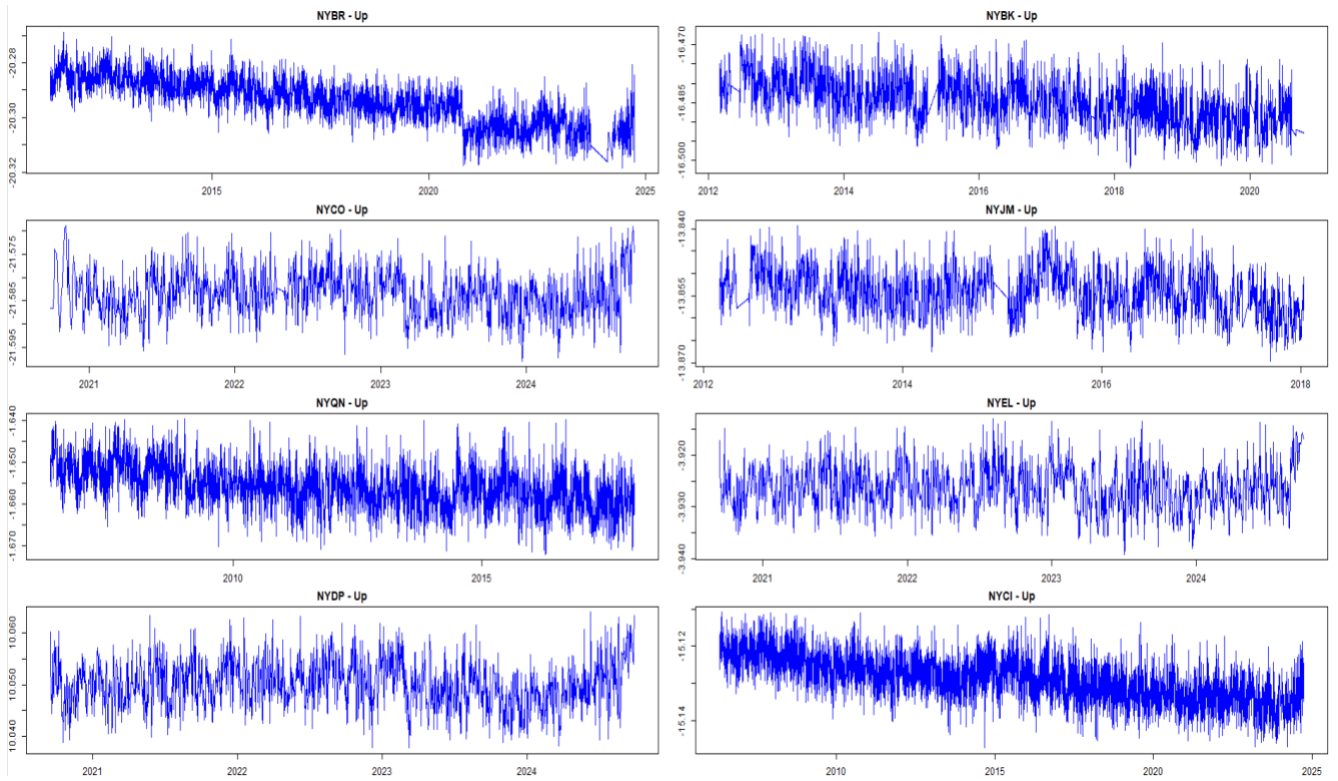
displacement, which coincides with regions being heavily dependent on water resources from the local aquifers.

Detailed time series analysis of the vertical displacement component for the 12 GPS stations revealed consistent trends of subsidence across nearly all locations. The stations revealing significant long-term downward trends are NYBK, NYBR, NYQN, SG06, MNPI, NYCI, NYRH, and NYEL (Figure 2). However, some of these stations like NYCI, NYRH, MNPI, and NYEL reveal slight indications of uplift events during the middle of 1997 and before 2025) (Figure 2). Some stations like NYCO, NYJM, NYPD, and ZNY1 reveal fluctuations of periods of subsidence followed by uplift and ending with a slight indication of subsidence and vice versa (Figure 2). Majority of these stations indicate significant or slight subsidence, shown at slightly lower magnitudes, and are mainly focused within New York City and at the western tip of Long Island, also known as Montauk Point (Figures 1 and 4). The spatial variation in the vertical displacement also encaptures what appears to be the beginning of an uplift event due to the expanded yearly range. Stations that indicate significant uplift are focused within the central areas of Long Island, including the western tip, as known as Brooklyn (Figures 1 and 4). These results underscore the influence of both natural geological processes, such as isostatic adjustments, and human factors, notably urbanization and groundwater extraction, on the observed subsidence trends. The clear spatial variation identified in this study provides critical insights necessary for regional planning and mitigation efforts.

Global Wavelet Spectrum indicating the up, north, and east components of Long Island revealed the oscillation that changed over time with the removal of any atmospheric noise that occurred in a time frame of any less than 365-days seasonality (Figure 3). The wavelet spectrum shows the average wavelet power for different periodicities in the vertical displacement of the GPS station. The wavelet spectrum of the up component reveals several peaks indicating dominant oscillation frequencies, meaning significant periodic movements in vertical displacement. The clustering of peaks at lower periods suggests that short-term variations (e.g., seasonal or sub-annual cycles) may be prominent in vertical land movement. The wavelet spectrum of the north component represents oscillations in the northward displacement of the GPS station, which remains relatively low, but some periodic signals are still evident, with the strongest periodicity appearing at higher values on the x-axis, suggesting long-term movements in the northward direction. The wavelet spectrum of the east component shows periodicities in the eastward displacement of the GPS station, which is slightly lower than that of the up component, but there is still a notable long-term trend, with a prominent peak at a high period suggesting a potential long-wavelength signal in eastward displacement, possibly linked to tectonic or subsidence processes.



Figure 1: Map displays the 12 stations, located at the east and the west of Long Island, studied in this research. Interactive map created in RStudio.



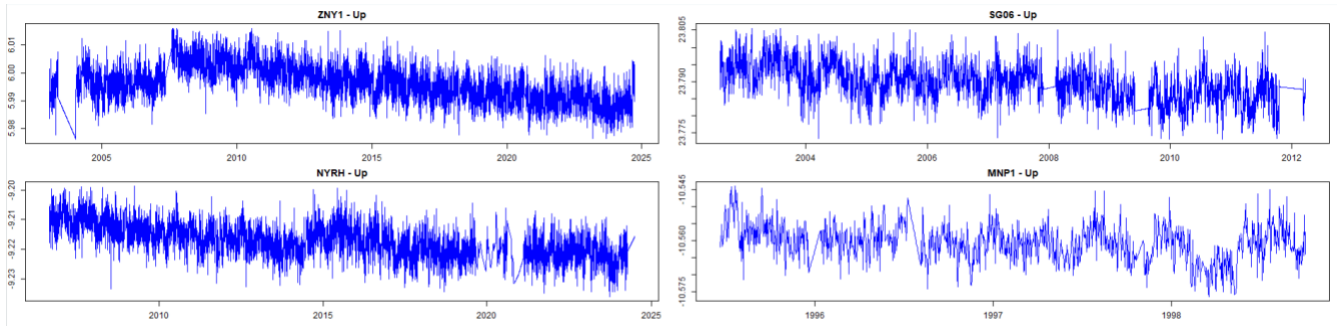


Figure 2: These graphs display the up components of each station and their oscillations within their various ranges. Some stations range from 1995-1998 and variations within the 2000s. Each station is labeled with their station name. The x-axis is time in years and the y-axis is the vertical displacement in meters (m).

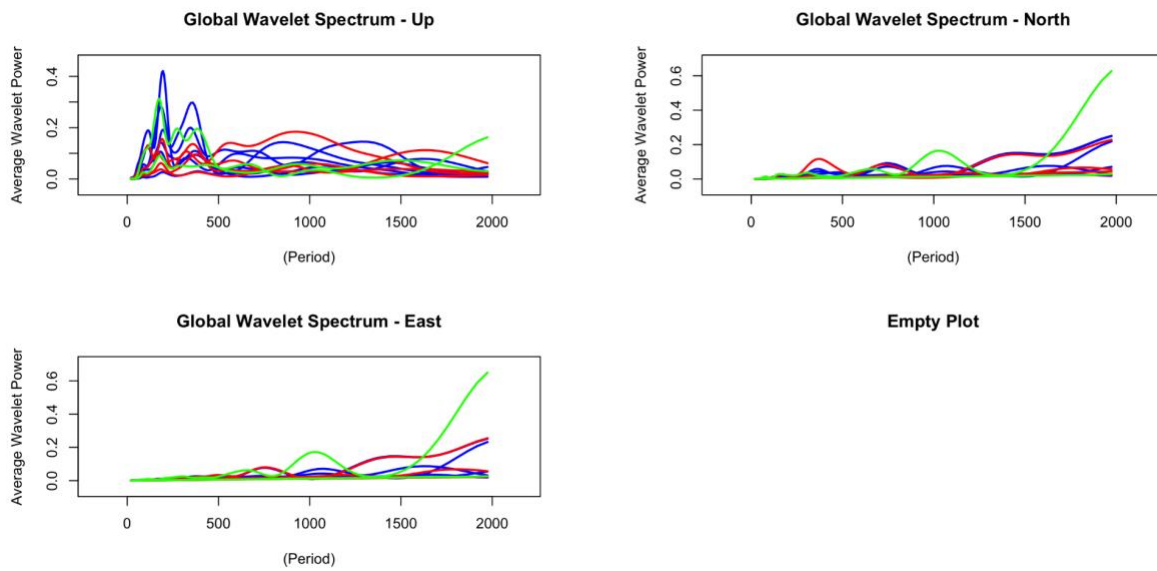


Figure 3: These graphs display the up, north, and east components of each station (various colored lines) and their oscillations within their various ranges. Some stations range from 1995-1998 and variations within the 2000s. The x-axis is the period (in days) and the y-axis is the vertical displacement in meters (m).

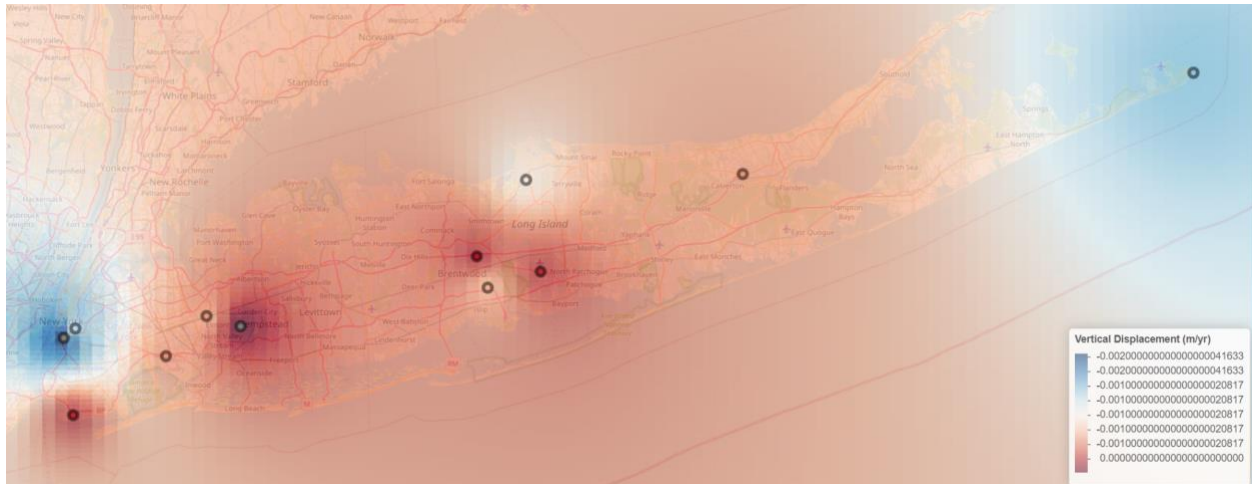


Figure 4: This GIS map displays the vertical displacement rates of each station and reveals potential areas of subsidence or uplift. The light red and white colored areas reveal areas of lower subsidence, the dark red colored areas reveal areas of uplift, and the blue colored areas reveal areas of high subsidence. Interactive map created in RStudio.

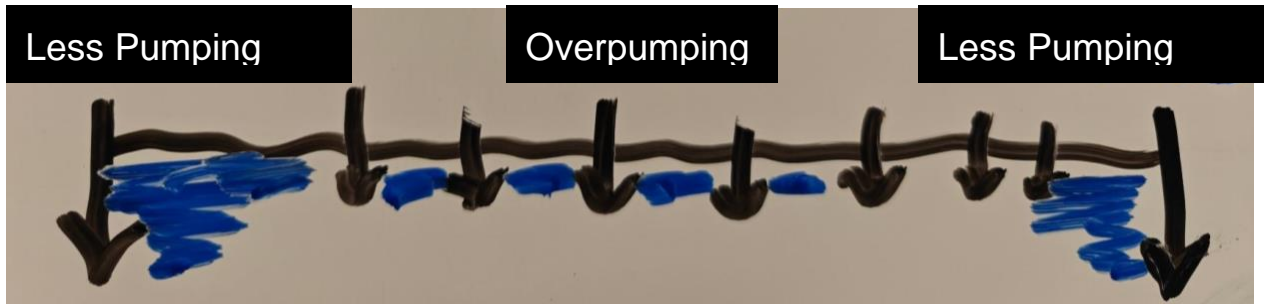


Figure 5: This image displays a suggested hypothesis as a conceptual sketch of the W-E cross-section of Long Island. The black arrows show the subsidence within the western, central, and eastern areas of Long Island. Longer arrows display higher subsidence rates and shorter arrows display lower subsidence rates. The blue drawings between the arrows represent aquifer presence and not real depth of aquifer. This image does not represent real dimensions.

## Discussion

This research investigates the continuation of the oscillations during long-term subsidence (including periods after 2020), with each station ranging from different time intervals, and what that will result in the isostasy of Long Island utilizing the entire available range of GPS data for vertical displacement analysis. Given that the study region belongs to a passive margin with low tectonic activity, long-term trends in the vertical up component are primarily influenced by non-tectonic factors. To estimate these trends, we applied a linear regression approach to the smoothed vertical displacement data for each station, computing annual vertical rates. This comprehensive time range shows a representation of long-term fluctuations in groundwater-related surface

deformation. Previous research has depicted that parts of Long Island are sinking over 3 centimeters per decade and on average about 1.6 millimeters per year (NASA Jet Propulsion Laboratory, 2023). Rather than limiting the analysis to a common time range across all stations, we prioritize understanding the overall vertical displacement trends and rates at each station individually. This approach offers a broader picture of ongoing isostatic response, even though stations vary in their operational time spans. To visualize regional patterns in land motion, a GIS-interpolated map was created using the average vertical displacement rates from all GPS stations across Long Island available from the University of Nevada, Reno Geodetic Laboratory. This map highlights spatial variability in subsidence and uplift, supporting interpretations of localized isostatic adjustment and human influences. Following the isostasy of Long Island, the weight of the large ice sheet caused the underlying land to subside and after the ice sheet melted then the land should have rebounded, uplifting the land to match its equilibrium point. However, during the GPS logging time, this uplift may have not occurred with the same intensity across Long Island possibly among other reasons due to the overpumped groundwater areas like within central Long Island, which shows signs of low subsidence rates. New York City has higher subsidence rates because of various large and tall infrastructures like buildings, roads, and power supplies. This may be attributable to the region's high construction density, associated loading on sediments, or infrastructural modifications. New York City, which primarily imports water from upstate and does not rely heavily on local aquifers for residential use, paradoxically displays pockets of greater subsidence. The quantity of groundwater within New York City's aquifer also adds weight to the underlying land, which can drag down the above area within it, since its aquifer contains more groundwater due to less pumping compared to the central Long Island aquifer system. The eastern end of Long Island also exhibits high subsidence rates but isn't as heavily populated as central and New York City. This may also contribute to the large quantity of groundwater within its aquifer since there are fewer people pumping groundwater and again this large amount of groundwater weighs down these specific regions. These groundwater overpumping effects can then lead to additional factors contributing to subsidence by creating leverage for sinkholes or landslides from weakened or dissolved sediments below the underlying surface.

The methods employed in this study extracted GPS displacement data to analyze vertical land motion using geostatistical analysis (Figure 2). Geostatistic analysis was then applied to investigate periodicity patterns in the vertical displacement, offering insights into land subsidence and uplift in response to isostatic adjustments. In our analysis, we applied Kolmogorov-Zurbenko (KZ) filtering with a 365-day window to preserve higher-frequency variations in the data. While previous research utilized a 730-day window, citing the lowest detectable frequency in spectral analysis, their results also indicated the presence of shorter periodicities, such as 365-day and 183-day cycles. By applying KZ filtering with a 365-day window, we removed variations with periods shorter than 365 days while preserving longer-term trends, including the 730-day frequency. This approach allowed us to retain more information on displacement rates at an annual scale, providing a clearer representation of long-term vertical motion while filtering out higher-frequency noise. Applying this filter proved highly effective in clarifying the long-term trends, ranging from 1995



to 2025, of subsidence across Long Island by significantly reducing the atmospheric noise and oscillations that typically obscure true geological displacement patterns. Atmospheric oscillations, which manifest prominently as short-term periodic variations, were initially visible through preliminary wavelet analyses and complicated the identification of genuine subsidence trends. Removing these noisy oscillations facilitated a clearer, more accurate depiction of vertical displacement rates, revealing subtle but significant subsidence patterns that otherwise would have been overshadowed by high-frequency atmospheric disturbances. The analysis highlights spatial variations in subsidence rates, notably higher in the areas of New York City and Montauk Point, and lower in the central region of Long Island including the western tip of Brooklyn. Mitigation strategies suggested include restricting groundwater extraction in vulnerable locations, utilizing lighter construction materials in future developments, and reconstructing existing structures to reduce surface loading, ultimately aiming to slow or prevent further land subsidence.

The Global Wavelet Spectrum presents multiple colored lines that suggest data from multiple GPS stations or different time series runs (Figure 3). Higher wavelet power at certain periods indicates recurring movements in land displacement, which could be driven by factors such as seasonal effects (e.g., groundwater fluctuations, temperature changes), tectonic activity, or subsidence (long-term periodicities). The Up component generally exhibits more pronounced oscillations compared to the horizontal (North and East) components. This is expected as vertical movement is often more sensitive to subsidence, uplift, and hydrostatic pressure changes. Applying the KZ filter enhances the ability to detect dominant periodic signals by removing short-term fluctuations that may obscure meaningful long-term oscillations.

The interpolated map underscores these spatial trends, clearly visualizing how subsidence intensifies near the western and eastern coastal regions while remaining comparatively lower in parts of central Long Island (Figure 4). This map is considered valid, as the long-term trends in GPS vertical displacement rates are not expected to change significantly over the 20-year data record. Given that the region is a passive margin with low tectonic activity, substantial variations would only be expected in the case of a major tectonic shift or significant new infrastructure development. However, the construction of high-rise buildings in the area occurred before GPS recording began, minimizing the likelihood of human influences on the observed displacement trends. Thus, the available GPS stations provide sufficient coverage to interpolate and construct a reliable displacement rate map. By contrast, New York City, which primarily imports water from upstate and does not rely heavily on local aquifers for residential use, paradoxically displays pockets of greater subsidence. This may be attributable to the region's high construction density, associated loading on sediments, or infrastructural modifications.

## **Conclusion**

There is a spatial variation in subsidence across Long Island, with intensified subsidence near coastal urban areas like New York City and at the easternmost place in Long Island, while

central Long Island exhibits relatively lower rates, driven by a combination of natural geological processes and possibly human-induced factors. The application of advanced data processing techniques, particularly the Kolmogorov-Zurbenko (KZ) filtering, significantly improved the accuracy and interpretability of GPS-derived displacement trends by effectively removing atmospheric noise while retaining data integrity. The wavelet spectrum analysis further identifies periodic fluctuations in vertical displacement, influenced by both seasonal and long-term environmental factors. These findings highlight the complexity of factors contributing to land motion—post-glacial isostatic readjustment, and human activities (e.g., pumping, construction, and natural sediment compaction). The gradient from urban centers outward is not uniform but instead reflects overlapping processes of geologic evolution and human intervention. This research also communicates the need for strategic groundwater management and urban planning to mitigate subsidence-related risks, including coastal flooding, infrastructure damage, and geohazards such as sinkholes and landslides. The GIS-interpolated displacement map provides a valuable tool for assessing vulnerable areas and guiding future land-use decisions. As sea levels continue to rise, understanding and addressing the ongoing subsidence of Long Island is critical for ensuring the long-term stability of coastal communities. Further integration of groundwater withdrawal data, soil compaction studies, and structural load analyses may clarify the interplay among these variables and improve future subsidence predictions.

### **Credit Authorship Contribution Statement**

Parag, A.: Literature, Editing, RStudio Coding, Writing- Abstract, Introduction, Methods, Results-Figures, Discussion, Conclusion; Marsellos, A.E.: Revision, Editing, RStudio Coding; Tsakiri, K.G.: KZ script insights

### **Acknowledgments**

*I would like to thank Dr. Antonios E. Marsellos and the Geology, Environment and Sustainability department at Hofstra University for providing me with the necessary tools to conduct this research. I would also like to thank Dr. Tsakiri for providing me with insights on KZ filtering script.*

### **References**

- Badger, T., Parag, A., Pelletier, A., DeRocchis, S., Marsellos, A. E., & Tsakiri, K. G. (2024). Investigating groundwater and landslides relationship using R: A study on Long Island's north shore. In *31st Conference on the Geology of Long Island and Metropolitan New York* (Abstract). Stony Brook University.
- Baker, A., et al. (2005). The Impact of Climate Change on Groundwater Resources: A Global Review. *Global and Planetary Change*, 47(2-4), 221-242. Elsevier. [https://doi.org/10.1016/S0921-8181\(01\)00150-3](https://doi.org/10.1016/S0921-8181(01)00150-3).
- Barrett, T., Dowle, M., Srinivasan, A., Gorecki, J., Chirico, M., Hocking, T., & Schwendinger, B. (2024). *data.table: Extension of data.frame*. R package version 1.16.4. Retrieved from <https://CRAN.R-project.org/package=data.table>.
- Bishop, P. (2007). Long-term landscape evolution: linking tectonics and surface processes. *Earth*

- Surface Processes and Landforms*, 32, 329-365. <https://doi.org/10.1002/esp.1493>.
- Bivand, R., Pebesma, E., & Gomez-Rubio, V. (2013). *Applied Spatial Data Analysis with R* (2nd ed.). Springer, NY. Retrieved from <https://asdar-book.org/>.
- Blewitt, G., & Lavallée, D. (2002). Effect of annual signals on geodetic velocity. *Journal of Geophysical Research*, 107(B7).
- Bloom, A. L. (1967). Pleistocene Shorelines: A New Test of Isostasy. *GSA Bulletin*, 78(12), 1477–1494. [https://doi.org/10.1130/0016-7606\(1967\)78\[1477:PSANTO\]2.0.CO;2](https://doi.org/10.1130/0016-7606(1967)78[1477:PSANTO]2.0.CO;2).
- Cheng, J., Schloerke, B., Karambelkar, B., & Xie, Y. (2024). *leaflet: Create Interactive Web Maps with the JavaScript 'Leaflet' Library*. R package version 2.2.2. Retrieved from <https://CRAN.R-project.org/package=leaflet>.
- Close, B., Zurbenko, I., & Sun, M. (2020). *kza: Kolmogorov-Zurbenko Adaptive Filters*. R package version 4.1.0.1. Retrieved from <https://CRAN.R-project.org/package=kza>.
- Davis, G. H. (1987). Land subsidence and sea level rise on the Atlantic Coastal Plain of the United States. *Environmental Geology and Water Sciences*, 10, 67–80. <https://doi.org/10.1007/BF02574663>.
- Dong, D., Fang, P., Bock, Y., Cheng, M. K., & Miyazaki, S. (2002). Anatomy of apparent seasonal variations from GPS-derived site position time series. *Journal of Geophysical Research*, 107(B4).
- Flavelle, C., & Rojanasakul, M. (2024, February 13). Flooding Isn't Just About Rising Seas. Groundwater Is a Threat, Too. *The New York Times*. Retrieved from <https://www.nytimes.com/interactive/2024/02/13/climate/flooding-sea-levels-groundwater.html?auth=login-google1tap&login=google1tap>.
- GPS data provided by the University of Nevada, Reno Geodetic Laboratory. Retrieved from [https://geodesy.unr.edu/gps\\_timeseries/tenv3/IGS14/](https://geodesy.unr.edu/gps_timeseries/tenv3/IGS14/).
- Gräler, B., Pebesma, E., & Heuvelink, G. (2016). Spatio-Temporal Interpolation using gstat. *The R Journal*, 8(1), 204-218.
- Grolemund, G., & Wickham, H. (2011). Dates and Times Made Easy with lubridate. *Journal of Statistical Software*, 40(3), 1-25. Retrieved from <https://www.jstatsoft.org/v40/i03/>.
- Hijmans, R. J. (2025). *raster: Geographic Data Analysis and Modeling*. R package version 3.6-31. Retrieved from <https://CRAN.R-project.org/package=raster>.
- Hope, J. H., Marsellos, A. E., & Tsakiri, K. G. (2024). High-frequency groundwater level fluctuations, underground erosion, potential sinkhole occurrences across Long Island, NY. In *31st Conference on the Geology of Long Island and Metropolitan New York* (Abstract). Stony Brook University.
- Larson, K. M., & van Dam, T. (2000). Measuring postglacial rebound with GPS and absolute gravity. *Geophysical Research Letters*, 27(23), 3925-3928.
- Moore, M., Brown, R., Thomas, M., Santella, K., Ballato, B., Marsellos, A. E., & Tsakiri, K. G. (2023). What can the local GPS network tell us about the Glacial Isostatic Adjustment of Long Island, NY? Retrieved from <https://ehs.stonybrook.edu/commcms/geosciences/about/LIG-Past-Conference-abstract-pdfs/2021-Abstracts/Moore.pdf>.
- Moritz, S., & Bartz-Beielstein, T. (2017). imputeTS: Time Series Missing Value Imputation in R. *The R Journal*, 9(1), 207-218. <https://doi.org/10.32614/RJ-2017-009>.
- NASA Jet Propulsion Laboratory. (2023, September 27). NASA-Led Study Pinpoints Areas of New York City Sinking, Rising. Retrieved from <https://www.jpl.nasa.gov/news/nasa-led-study-pinpoints-areas-of-new-york-city-sinking-rising/>.

- National Oceanic and Atmospheric Administration. (n.d.). Sea level rise viewer. NOAA Office for Coastal Management. Retrieved from <https://coast.noaa.gov/digitalcoast/tools/slr.html>.
- Pebesma, E. J. (2004). Multivariable geostatistics in S: the gstat package. *Computers & Geosciences*, 30, 683-691.
- Pebesma, E., & Bivand, R. (2005). Classes and methods for spatial data in R. *R News*, 5(2), 9-13. Retrieved from <https://CRAN.R-project.org/doc/Rnews/>.
- R Core Team. (n.d.). *The Comprehensive R Archive Network (CRAN)*. R Foundation for Statistical Computing. Retrieved March 31, 2025, from <https://cran.r-project.org/>
- Roesch, A., & Schmidbauer, H. (2018). *WaveletComp: Computational Wavelet Analysis*. R package version 1.1. Retrieved from <https://CRAN.R-project.org/package=WaveletComp>.
- Shepard, C. C., Agostini, V. N., Gilmer, B., et al. (2012). Assessing future risk: quantifying the effects of sea level rise on storm surge risk for the southern shores of Long Island, New York. *Natural Hazards*, 60, 727–745. <https://doi.org/10.1007/s11069-011-0046-8>.
- Taniguchi, M. (2001). Evaluation of the Groundwater Recharge Rate through the Unsaturated Zone Based on the Temporal Change in Temperature. *Ecological Modelling*, 138(1-3), 291-301. [https://doi.org/10.1016/S0921-8181\(01\)00150-3](https://doi.org/10.1016/S0921-8181(01)00150-3).
- Tsakiri, K.G., Zurbenko, I.G., 2011a. Effect of noise in principal component analysis. *J. Stat. Math.* 2, 40.
- Tsakiri, K.G., Zurbenko, I.G., 2011b. Prediction of ozone concentrations using atmospheric variables. *Air Qual. Atmos. Health* 4, 111–120.
- Tsakiri, K., Marsellos, A., Kapetanakis, S., 2018. Artificial Neural Network and Multiple Linear Regression for Flood Prediction in Mohawk River, New York. *Water* 10, 1158.
- U.S. Geological Survey. (n.d.). *Land subsidence*. The Water Science School. Retrieved [date], from <https://www.usgs.gov/special-topics/water-science-school/science/land-subsidence#overview>.
- Vincent Y. S. Cheng, Ali Saber, Carlos Alberto Arnillas, Aisha Javed, Agnes Richards, & George B. Arhonditsis. (2021). Effects of hydrological forcing on short- and long-term water level fluctuations in Lake Huron-Michigan: A continuous wavelet analysis. *Journal of Hydrology*, 603, Part D. <https://doi.org/10.1016/j.jhydrol.2021.127164>.
- Vivien Gornitz, Stephen Couch, & Ellen K. Hartig. (2001). Impacts of sea level rise in the New York City metropolitan area. *Global and Planetary Change*, 32(1), 61-88.
- Wickham, H., François, R., Henry, L., Müller, K., & Vaughan, D. (2023). *dplyr: A Grammar of Data Manipulation*. R package version 1.1.4. Retrieved from <https://CRAN.R-project.org/package=dplyr>.
- Wickham, H., & Henry, L. (2025). *purrr: Functional Programming Tools*. R package version 1.0.4. Retrieved from <https://CRAN.R-project.org/package=purrr>.
- Yang, W., Zurbenko, I., 2010. Nonstationarity. *Wiley Interdiscip. Rev. Comput. Stat.* 2, 107–115.
- Zeileis, A., & Grothendieck, G. (2005). zoo: S3 Infrastructure for Regular and Irregular Time Series. *Journal of Statistical Software*, 14(6), 1-27. <https://doi.org/10.18637/jss.v014.i06>.